Chinese Journal of Electronics
Vol.32, No.4, July 2023

Enhancing Network Throughput via the Equal Interval Frame Aggregation Scheme for IEEE 802.11ax WLANs

ZHU Yihua and XU Mengying

(*School of Computer Science and Technology, Zhejiang University of Technology, Hangzhou 310023, China*)

Abstract — Frame aggregation is fully supported in the newly published IEEE 802.11ax standard to improve throughput. With frame aggregation, a mobile station combines multiple subframes into an aggregate MAC service data unit (A-MSDU) or an aggregate MAC protocol data unit (A-MPDU) for transmission. It is challenging for a mobile station in 802.11ax WLANs to set an appropriate number of subframes being included in an A-MSDU or A-MPDU. This problem is solved in this paper by the proposed equal interval frame aggregation (EIFA) scheme which lets a mobile station aggregate at most k subframes at a fixed time period of T. A novel Markov model is developed for deriving the probability of number of subframes in the data buffer at the mobile station, resulting in the throughput and packet delay in the EIFA. Moreover, the optimization problem of maximizing the throughput with the constraint on delay is formulated, and its solution leads to the optimal pair of parameters k and T for improving throughput in the EIFA scheme. Simulation results show the EIFA has a higher throughput than the ones in which the mobile station chooses the minimum, the maximum, or a random number of subframes.

Key words — IEEE 802.11ax standard, Frame aggregation, WLAN, Throughput, Markov model, MAC.

I. Introduction

The Internet of things (IoT) plays a key role in collecting data from the environment. Wireless local area networks (WLANs) and wireless sensor networks (WSNs) are main components of the IoT. Typically, WLAN and WSN adopt IEEE 802.11 standard [1] and IEEE 802.15.4 standard [2] in the medium access control (MAC) and the physical layers, respectively. The popular Wi-Fi is based on the IEEE 802.11 standard.

Due to IEEE 802.15.4 standard targeting at low power, data rates applied at nodes in the WSNs are quite low, usually having tens of Kbps. In order to deliver data in a higher rate, some WSN applications accommodate Wi-Fi technology. The examples include: Wi-Fi enabled sensors were introduced [3]; Wi-Fi chipsets were applied in monitoring temperature, humidity, volatile organic compounds and miniature dust particles [4]; Wi-Fi embedded network processors were used in monitoring heart rate [5]; and Wi-Fi module was used in the car that can sense obstruction, temperature, gas, fire, etc. [6]. In a word, the IEEE 802.11 standard is frequently applied in the WSN applications.

In fact, the IEEE 802.11 family of standards has acted as one of the most popular technologies for wireless connectivity. Nodes in the IEEE 802.11 standard based WLAN are termed as mobile stations (STAs). Since the birth of the first IEEE 802.11 standard [1] issued in 1997, members of the 802.11 family are increasing. The newest member is the IEEE 802.11ax standard [7], released in May 2021, called Wi-Fi 6, which introduces some new features, including the orthogonal frequency division multiple access (OFDMA) that supports the STAs to simultaneously transmit over multiple resource units (RUs) [8].

A MAC frame, namely MAC protocol data unit (MPDU), carries MAC service data unit (MSDU). More specifically, MPDU consists of MSDU and the MAC header and the MAC tail. Here, the header and the tail are overhead. Clearly, in the case when the size of the MAC header and tail is close to or greater than that of MSDU, efficiency of channel usage is low.

Apart from the MAC header and tail, channel contention (e.g., backoff) and acknowledgement (ACK) of frame also yield overhead. To reduce overhead, frame

Manuscript Received Aug. 21, 2022; Accepted Jan. 6, 2023. This work was supported by the National Natural Science Foundation of China (61772470, 61432015) and the National Key R&D Program of China (2019YFD0901605).
 DOI:10.23919/cje.2022.00.282

aggregation is introduced in IEEE 802.11n standard [9] in 2009 and extended by the newest Wi-Fi 6 in 2021 [7]. With frame aggregation, a STA encapsulates multiple short frames into one longer frame so that the multiple short frames share the header and tail of the MAC frame, the preamble and header of the physical layer, the time consumed in channel contention, and ACK frame. It was reported that efficiency of channel usage and network throughput can be considerably improved when the STAs adopt frame aggregation.

Before the birth of Wi-Fi 6, the MPDUs must all be of the same 802.11e quality of service (QoS) access category when A-MPDU frame aggregation is used, and voice MPDUs cannot be mixed with best effort or video MPDUs within the same aggregated frame. Wi-Fi 6, however, introduces multi-traffic identifier aggregated MPDU (Multi-TID A-MPDU) that supports the aggregation of frames from multiple traffic identifiers (TIDs). It is Wi-Fi 6 that has the capability of mixing MPDUs, i.e., it can integrate frames from the same or different QoS access categories. The ability of combining MPDUs from different QoS traffic classes allows 802.11ax radios to aggregate more efficiently by transmitting over multiple RUs, thus reducing overhead and increasing overall network efficiency.

We notice that the existing frame aggregation schemes have one or more of the following shortcomings. First, they do not take into account the OFDMA mechanism, a new feature introduced in the newest IEEE 802.11ax standard, which supports simultaneous transmission over multiple RUs.

Second, the IEEE 802.11ax standard only defines the range of the number of subframes (NoS), but the STAs do not have the knowledge of how many subframes should be included in generating a longer frame. Here, subframes are the short frames being aggregated. Third, in the case when traffic to a STA is intermittent, the STA needs to wait for multiple subframes to arrive and then aggregate them to produce a longer frame. Obviously, a shorter waiting time may result in only a few subframes being aggregated, which may decrease efficiency of channel usage, whereas a longer waiting time causes a longer packet delay although it helps in aggregating more subframes to improve efficiency of channel usage. Obviously, it is time-consuming in practice for a STA to test all the NoSs with different TIDs for the best NoS.

In summary, it is urgent to design a frame aggregation scheme that both takes into account the OFDMA mechanism and supports the STAs in the 802.11ax WLAN to find the optimal pair of NoS and waiting time so that efficiency of channel usage is enhanced. This is the motivation of our work.

This paper has the contributions as follows:

- We propose the equal interval frame aggregation (EIFA) scheme that aims to improve throughput. In the EIFA, there are two parameters k and T. With the EIFA scheme, each STA aggregates at most k subframes in its data buffer at a fixed time period of T to generate a longer frame. It should be stressed that the subframes in the EIFA scheme can be with different TIDs. This characteristic differs from the existing frame aggregation schemes based on the IEEE 802.11 standards prior to Wi-Fi 6.
- We develop a novel Markov chain to model the EIFA, from which we derive the probability of the number of the subframes in the data buffer at the STA. Then, we derive the throughput and delay in the EIFA. In addition, we formulate the optimization problem that maximizes the throughput with respect to the pair of parameters k and T under delay constraint. The solution to the optimization problem leads to the optimal values of the parameters k and T, which are applied in the EIFA scheme.
- Simulation results show that the proposed EIFA achieves a higher throughput than the ones in which a STA chooses the minimum NoS, the maximum NoS, or a random NoS.

The rest of the paper is organized as follows. The related researches are surveyed in Section II. We outline frame aggregation and present the EIFA with its Markov model in Section III, formulate the optimization problem in Section IV, evaluate the performance of the EIFA via simulation in Section V, and conclude the paper in Section VI.

II. Related Work

As previously mentioned, the OFDMA mechanism is one of the new features in the newly-published IEEE 802.11ax standard, which allows access point (AP) to divide wireless channel into smaller chunks (i.e., RUs) and allocate them to different users. The OFDMA mechanism has attracted much interest in research community. Kotagiri *et al.* [10] proposed a distributed RU selection method using convolutional neural network based deep reinforcement learning to improve throughput and latency. Xie *et al.* [11] developed a multi-dimensional busy-tone arbitration mechanism to reduce collisions among STAs contending for the same RU. Zheng *et al.* [12] studied the OFDMA-based random access backoff and presented the retransmission number aware channel access (RNACA) scheme for IEEE 802.11ax-based WLAN, which lets the STA intending to retransmit a frame make decision on whether to double its OFDMA contention window size or not by using a probability resulting from the number of retransmissions, number of RUs, and number of STAs. To avoid collision in the uplink OFDMA random access (UORA), Lee *et al.* [13] proposed the method with non-orthogonal multiple access (NOMA). Lanante *et al.* [14] equipped UORA with carrier sensing capability and developed the hybrid UORA OFDMA access mechanism to reduce collisions. Cheng *et al.* [15] presented an analytical model to investigate the performance of UORA in transient condition under burst arrivals with arbitrary distribution, which leads to access success probability, average access delay, cumulative distribution function (CDF) for the number of transmissions, and utilization of UORA. In addition, Ghanem *et al.* [16] considered resource allocation for multi-user downlink multiple input single output OFDMA system. And Khoramnejad *et al.* [17] investigated load management, power and admission control in downlink cellular OFDMA networks.

Although frame aggregation is designed for 802.11 WLAN, it has been applied in WSN. Xiao *et al.* [18] proposed an opportunistic data aggregation algorithm to support the data collection in low-duty-cycle WSNs with unreliable links.

Lin *et al.* [19] proposed an analytical model to study the performance of the MAC protocol by using the two frame aggregation techniques, namely MPDU aggregation (A-MPDU) and MSDU aggregation (A-MSDU), under uni-directional and bi-directional data transfer. Kowsar *et al.* [20] analyzed performance of combined A-MSDU and A-MPDU via NS-3 simulation. Abdallah *et al.* [21] developed a framework for jointly selecting the data rate, the multiple input multiple output (MIMO) mode and the frame aggregation configuration at the AP using subcarrier-level channel state information. Assasa *et al.* [22] considered impact of the traffic patterns in the wireless network on frame aggregation, and then they presented a waiting policy for the uplink case that either waits for a minimum number of packets or for a maximum amount of time, whichever comes first.

Nomura *et al.* [23] proposed an efficient frame aggregation scheme that improves system throughput and decreases frame error rate for downlink multi-user MIMO transmissions in IEEE 802.11ac WLANs.

Charfi *et al.* [24] proposed a scheduling algorithm based on urgency delay and an adaptive frame aggregation technique to obtain an optimal trade-off between maximizing throughput and minimizing delay.

Zhou *et al.* [25] proposed an adaptive frame length aggregation scheme for vehicular ad hoc networks (VANETs), aiming at improving transmission efficiency and increasing data throughput. Yazid *et al.* [26] modeled the 802.11ac station enabling A-MPDU and spatial multiplexing, and then computed the throughput and the overhead in the 802.11ac network. Saldana *et al.* [27] explored the throughput versus latency tradeoff in the context of central controlled solutions. Saldana *et al.* [28] proposed an algorithm for the dynamic tuning of the maximum size of aggregated frames in 802.11 WLANs, which allows the network manager to find the optimal balance between throughput and latency.

Abedi *et al.* [29] focused on finding the optimal length of an A-MPDU and developed a standard compliant, practical, near-optimal frame aggregation algorithm (PNOFA) in order to maximize throughput. Morimoto *et al.* [30] analyzed throughput and delay in full-duplex WLANs with frame aggregation. Liu *et al.* [31] proposed an adaptive frame length aggregation strategy with remaining delay limit in VANETs. Kim *et al.* [32] analyzed how different overhead components impact the efficiency of multi-user transmission and presented a scheme for constructing a multi-user frame with the optimal length to maximize transmission efficiency. Liu *et al.* [33] optimized the number of the aggregated sub-MAC protocol data units to maximize the throughput of the two-level frame aggregation according to the subframe size, the maximum aggregation level and the real-time channel bit-error-rate (BER). Suzuki *et al.* [34] constructed an optimization problem that maximizes theoretical throughput considering bit error in A-MSDU under the IEEE 802.11ac standard and proposed a scheme to determine the optimal subframe sets through an exhaustive search for both A-MPDU and A-MSDU.

Kim *et al.* [35] proposed an analytical model based on an enhanced discrete time Markov chain to describe the post-backoff behavior due to frame aggregation, and evaluated the throughput performance. Seytnazarov *et al.* [36] proposed a Markov chain model to estimate the average aggregation size resulting from block acknowledgement window operations under noisy channel conditions, and the obtained average aggregation size was used in enhancing the performance of the aggregation-enabled WLANs. Jabri *et al.* [37] adopted Markov model for 802.11n MAC layer to remedy the drawback in the available analytical models in which the impact of the block ACK window limit on the aggregated frame size is ignored. Lu *et al.* [38] presented the timely data delivery (TDD) scheme and a Markov chain model for the TDD to reduce packet delay for energy-harvesting IoT devices.

The EIFA scheme proposed in this paper differs from the existing schemes in that: 1) NoS and waiting time are jointly optimized, which yields the optimal pair of the parameters to maximize network throughput; and 2) The OFDMA mechanism introduced in the newest IEEE 802.11ax standard is considered.

III. The EIFA Scheme with Mathematics Model

Frame aggregation is classified by one-level and two-level. The one-level frame aggregation consists of A-MSDU and A-MPDU, shown in Fig.1(a) and (b), respectively [39], where DA and SA stand for destination address and source address, respectively. The two-level frame aggregation is shown in Fig.1(c), which combines A-MSDU and A-MPDU.

IEEE 802.11ax standard limits the maximum number of MPDU subframes to 64 [7]. It, however, leaves the optimal NoS unsolved. This brings a challenge to the STAs that need suitable NoS in frame aggregation. We will address the problem via a Markov model in the next section.

This paper focuses on one-level frame aggregation.

1. The EIFA Scheme

In this paper, we study the WLAN in which all STAs adopt IEEE 802.11ax standard in their MAC and physical layers and the STAs apply the proposed EIFA scheme in delivering data.

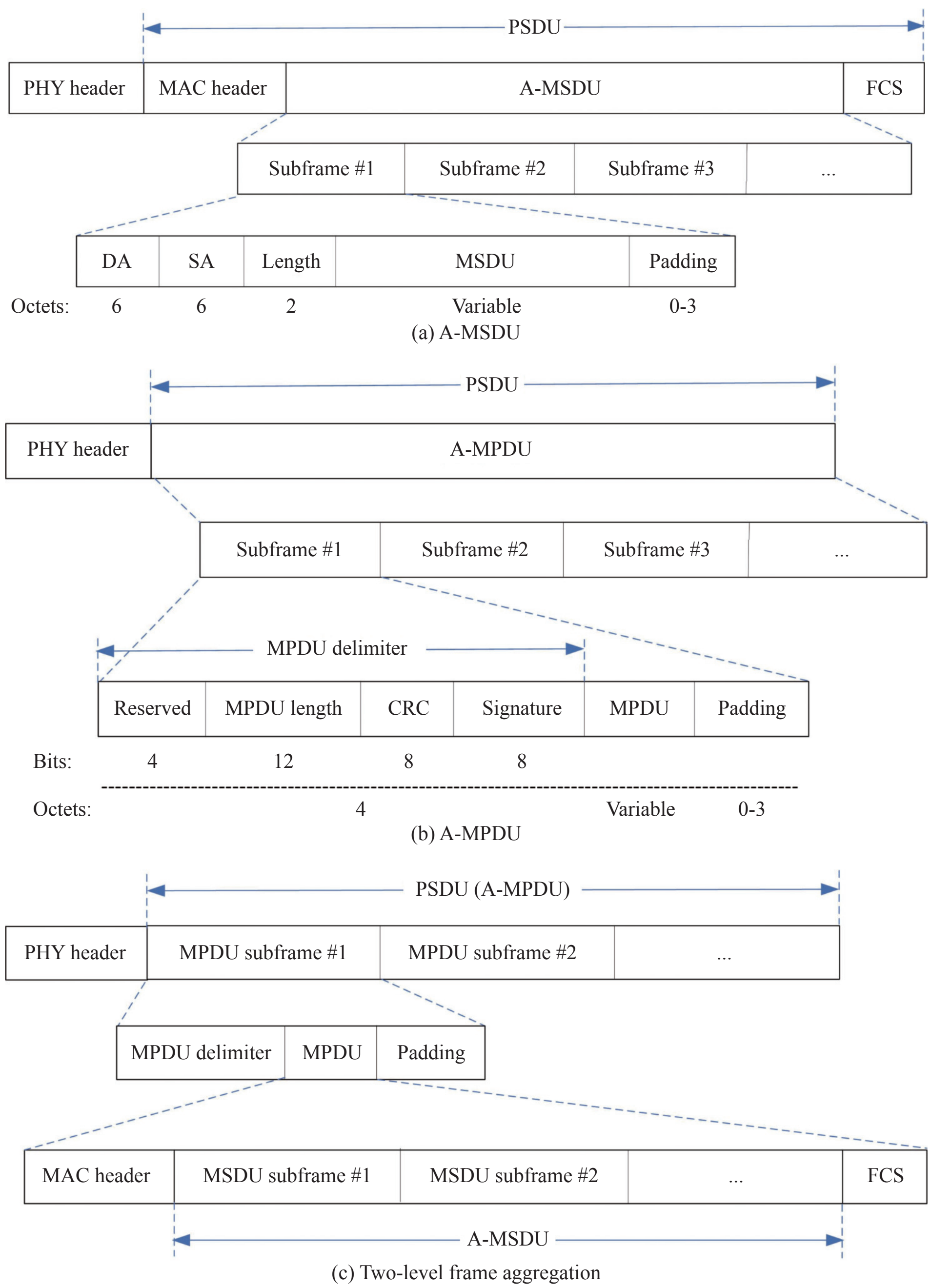

Fig. 1. Two levels of frame aggregation.

In the sequel, we refer to the frame generated by aggregating subframes as a "long frame." Accordingly, the subframes being aggregated are termed as "short frames."

Our EIFA scheme is characterized by the following features:

1) At every fixed time interval of T, called aggregation period below, a STA in the WLAN aggregates at most k short frames to generate one long frame;

2) Frame aggregation begins at the end of an aggregation period;

3) The generated long frame is transmitted upon completion of frame aggregation; and

4) Only one long frame is generated and transmitted in an aggregation period.

The EIFA scheme is illustrated in Fig.2, where the proposed EIFA scheme resides in the MAC layer in the open system interconnection (OSI) reference model. The EIFA uses the data buffer to keep the traffic from the upper layer, and it aggregates at most k short frames to generate one long frame at every aggregation period. The long frame is passed down to the physical layer. The green line stands for the boundary of the EIFA scheme.

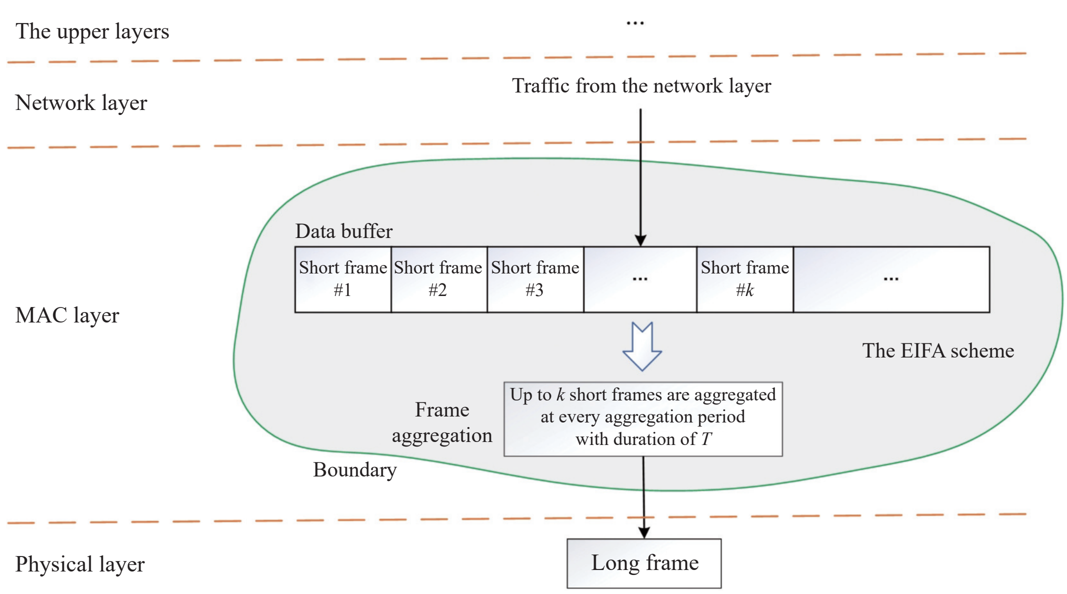

Fig. 2. Diagram of the EIFA.

Recall that IEEE 802.11ax standard, or Wi-Fi 6, aims at high efficiency (HE) [7], which differs from IEEE 802.11ac standard (i.e., Wi-Fi 5) targeting at very high throughput (VHT). Only the HE STAs can take advantage of the new features introduced in Wi-Fi 6, including the OFDMA mechanism. Therefore, it is required that the STAs operating with the EIFA be HE stations so that the EIFA can achieve the best performance. In the case when each of the STAs with the EIFA is not HE station, the EIFA cannot benefit from the new features in Wi-Fi 6.

2. Mathematics model for the EIFA scheme

In this section, we use Markov chain to model the EIFA scheme in Fig.2. The Markov model aims at deriving the statistics (i.e., throughput and packet delay, etc.) under the EIFA scheme, from which we obtain the optimal pair of parameters k and T for the proposed EIFA scheme by solving the optimal problem that maximizes the throughput subject to the constraint on the packet delay.

1) Assumptions: Given a STA in the WLAN, we assume that the short frame arrivals at the data buffer of the STA obey a Poisson process with rate of λ [40], [41].

In order to avoid the data buffer growing without bound, we require the aggregation period of T to satisfy

$$T < \frac{k}{\lambda} \tag{1}$$

The reason is explained as follows. In the EIFA scheme, one long frame, which consists of at most k short frames, is transmitted in an aggregation period of T. Hence, the transmission rate of long frame, i.e., the number of long frames being transmitted per unit of time, is $1/T$. Equivalently, the transmission rate of short frame is up to k/T. Therefore, we need the short frame transmission rate being greater than the short frame arrival rate λ. That is, $k/T > \lambda$, leading to (1).

2) State probabilities: Let a_n denote the probability that there are exact n short frames arriving at the

STA during an aggregation period with duration of T. Then, we have [42]

$$a_n = \frac{(\lambda T)^n}{n!}\mathrm{e}^{-\lambda T},\ n = 0, 1, \dots \tag{2}$$

The STA is said to be in state S_j if there are j short frames in the data buffer at the STA ($j = 0, 1, \dots$). Then, the state space is $\Omega = \{S_0, S_1, \dots\}$. Let state probability $P_j = \Pr\{S_j\}$, which is the probability of the event that the STA is in state $S_j \in \Omega$. Thus, it holds that $\sum_{S_j\in\Omega} P_j = 1$. Equivalently,

$$\sum_{j=0}^{\infty} P_j = 1 \tag{3}$$

In addition, for two states $S_i, S_j \in \Omega$, we introduce notation $q_{i,j} = \Pr\{S_j|S_i\}$ to represent the probability of transition from S_i to S_j.

Then, we consider the state transitions occur at the ends of aggregation periods, with the assumption that the STA is initialized to be in state S_0.

State transitions related to S_0 are illustrated in Fig.3(a), which is explained as follows. We first consider the state transitions starting from S_0. During an aggregation period with length of T, the number of short frames arriving at the STA is possibly $0, 1, \dots, k, \dots$ with probability of $a_0, a_1, \dots, a_k, \dots$, respectively. Due to the fact that at most k short frames are aggregated to form one long frame being transmitted at the end of the aggregation period, the event that the number of frame arrivals being $0, 1, \dots,$ or k, which happens with probability of $\sum_{i=0}^{k} a_i$, does not change the STA's state. That is, all the arrived short frames are aggregated and transmitted so that no short frame is left at the data buffer. Hence, the transition from state S_0 to itself happens with probability of $\sum_{i=0}^{k} a_i$. However, $k+1, k+2, \dots$ frame arrivals cause the STA's state to be $S_1, S_2, \dots$ with probability $a_{k+1}, a_{k+2}, \dots$, respectively. Then, we consider state transitions that end at S_0. In the case when $i = 1, 2, \dots, k$, the STA's state changes from S_i to S_0 when no more than $k-i$ frames arrives at the STA, which occurs with probability of $\sum_{j=0}^{k-i} a_j$, because no frame stays at the data buffer after the aggregation process that consumes at most k short frames. Clearly, transition from states $S_{k+1}, S_{k+2}, \dots$ to S_0 does not occur in one frame aggregation period under the proposed EIFA scheme.

Thus, transition probabilities out of state S_0 can be represented by

$$q_{0,j} = \begin{cases} \sum_{i=0}^{k} a_i, & j = 0 \\ a_{k+j}, & j = 1, 2, \dots \end{cases} \tag{4}$$

Similarly, state transitions related to S_1 and S_k are shown in Fig.3(b) and (c), respectively. Moreover, those related to state $S_j (j > k)$ are shown in Fig.3(d). The explanation of Fig.3(b)–(d) is similar to Fig.3(a), which is omitted.

From Fig.3, we obtain all state transition probabilities as follows:

1) For $i = 0, 1, \dots, k$,

$$q_{i,j} = \begin{cases} \sum_{h=0}^{k-i} a_h, & j = 0 \\ a_{k+j-i}, & j = 1, 2, \dots \end{cases} \tag{5}$$

2) For $i = k+1, k+2, \dots$,

$$q_{i,j} = \begin{cases} 0, & j = 0, 1, \cdots, i-k-1 \\ a_{j-i+k}, & j = i-k, i-k+1, \dots \end{cases} \tag{6}$$

Now, we start deriving the state probability $P_j = \Pr\{S_j\}, j = 0, 1, \dots$. The event of the STA being in state $S_j \in \Omega$ is equivalent to the union of the following events:

1) The STA is originally in state S_j and then it remains the same state in an aggregation period, which occurs with probability of $P_j\, q_{j,j}$; and

2) The STA is originally in state $S_h \in \Omega$ other than S_j (i.e., $h \neq j$) and then it changes its state from S_h to S_j, which occurs with probability of $P_h\, q_{h,j}, S_h \in \Omega - \{S_j\}$.

Thus, we have

$$P_j = \sum_{h=0}^{\infty} P_h q_{h,j},\ \ j = 0, 1, \dots \tag{7}$$

The above equations can be expressed as follows:

$$\mathbb{A}_\infty \vec{P}_\infty = \vec{0}_\infty \tag{8}$$

where $\vec{P}_\infty = (P_0, P_1, \dots, P_n, \dots)^{\mathrm{T}}$, $\vec{0}_\infty$ is a vector with infinite elements being 0 s, and

$$\mathbb{A}_\infty = \begin{bmatrix} q_{0,0}-1 & q_{1,0} & \cdots & q_{n,0} & \cdots \\ q_{0,1} & q_{1,1}-1 & \cdots & q_{n,1} & \cdots \\ \vdots & \vdots & \ddots & \vdots & \ddots \\ q_{0,n} & q_{1,n} & \cdots & q_{n,n}-1 & \cdots \\ \vdots & \vdots & \ddots & \vdots & \ddots \end{bmatrix} \tag{9}$$

Equation (3) indicates that the infinite series $\sum_{j=0}^{\infty} P_j$ converges to 1, which requires $\lim_{n\to\infty} P_n = 0$. As a result, for any small real number ε, say $\varepsilon = 10^{-4}$, there exists a sufficient large integer M so that

$$P_{M+1} + P_{M+2} + \cdots < \varepsilon \tag{10}$$

which indicates that the probability of the data buffer

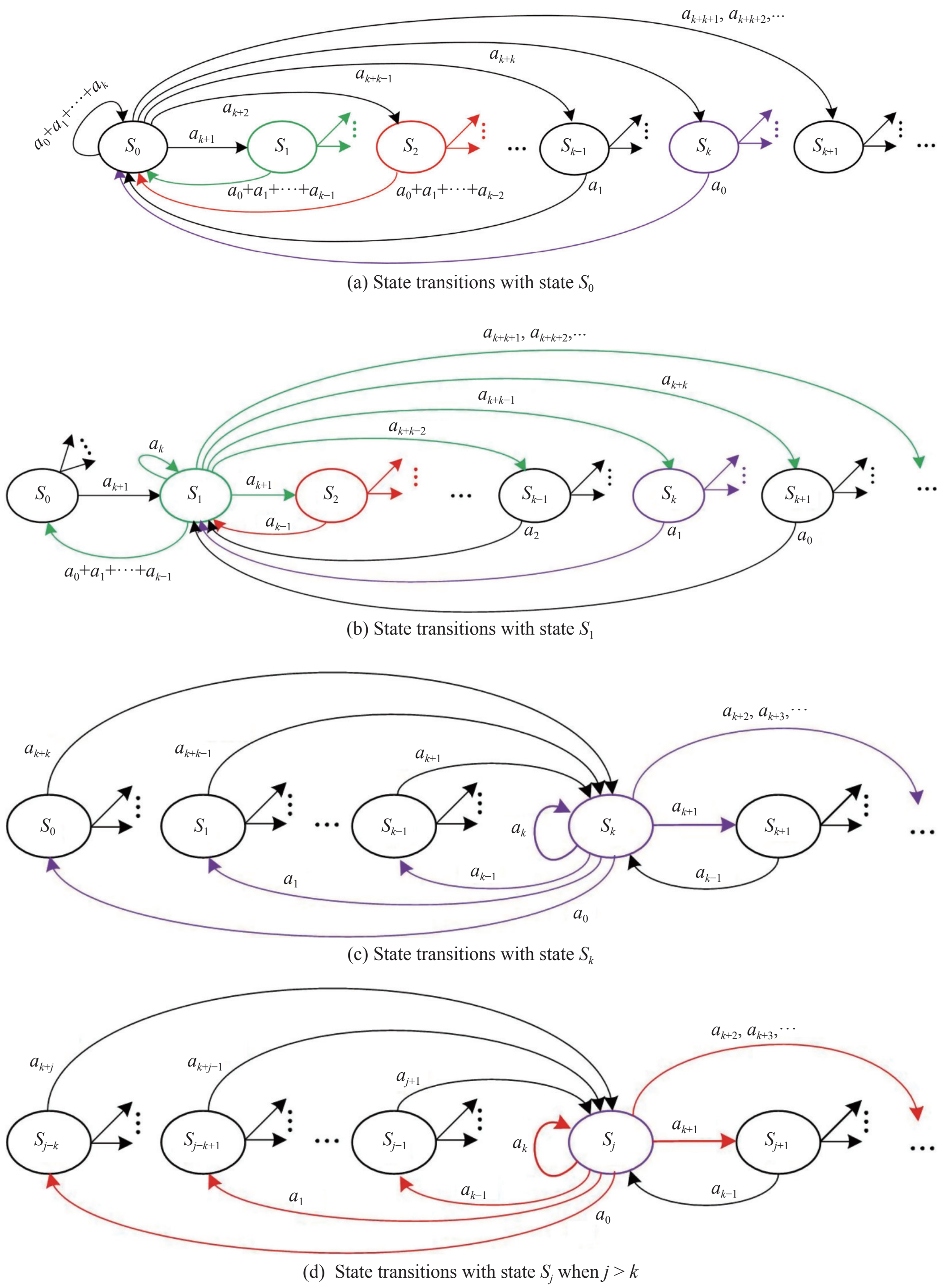

Fig. 3. State transition diagram.

having more than M short frames can be ignored. Equivalently,

$$\sum_{j=0}^{M} P_j \approx 1 \tag{11}$$

with precision of ε.

Therefore, with this M, the set of infinite equations in (8) can be approximated with precision of ε by the following $M+1$ equations:

$$\tilde{\mathbb{A}}_M \vec{P}_M = \vec{0}_M \tag{12}$$

In (12), both $\vec{P}_M$ and $\vec{0}_M$ are $(M+1)$-dimension vectors and $\tilde{\mathbb{A}}_M$ is an $(M+1)\times(M+1)$ matrix, which are defined as follows: $\vec{P}_M = (P_0, P_1, \ldots, P_M)^{\mathrm{T}}$ and $\vec{0}_M$ has all elements of 0 s, and

$$\tilde{\mathbb{A}}_M = \begin{bmatrix} q_{0,0}-1 & q_{1,0} & \cdots & q_{M,0} \\ q_{0,1} & q_{1,1}-1 & \cdots & q_{M,1} \\ \vdots & \vdots & \ddots & \vdots \\ q_{0,M} & q_{1,M} & \cdots & q_{M,M}-1 \end{bmatrix}. \tag{13}$$

Usually, matrix $\tilde{\mathbb{A}}_M$ is not fully ranked, which may cause the problem that the set of equations in (12) does not have unique solution. Fortunately, this problem can be remedied by replacing one of the equations, say the first equation, with (11). Then, we have

$$\mathbb{A}_M \vec{P}_M = \vec{b}_M \tag{14}$$

where $\vec{b}_M = (1, 0, 0, \ldots, 0)^{\mathrm{T}}$ and the $(M+1)\times(M+1)$ matrix $\mathbb{A}_M$ is

$$\mathbb{A}_M = \begin{bmatrix} 1 & 1 & \cdots & 1 \\ q_{0,1} & q_{1,1}-1 & \cdots & q_{M,1} \\ \vdots & \vdots & \ddots & \vdots \\ q_{0,M} & q_{1,M} & \cdots & q_{M,M}-1 \end{bmatrix} \tag{15}$$

Using (5) and (6) in (15), we obtain

$$\mathbb{A}_M = \mathbb{B}_{M1} - \mathbb{B}_{M2} \tag{16}$$

Here, both $\mathbb{B}_{M1}$ and $\mathbb{B}_{M2}$ are $(M+1)\times(M+1)$ matrices, where

$$\mathbb{B}_{M2} = \mathrm{diag}\{0, \underbrace{1, 1, \cdots, 1}_{M}\} \tag{17}$$

and $\mathbb{B}_{M1}$ consists of two $(M+1)$-row matrices $\mathbb{B}_{M11}$ and $\mathbb{B}_{M12}$ as

$$\mathbb{B}_{M1} = \Big[\mathbb{B}_{M11} : \mathbb{B}_{M12}\Big] \tag{18}$$

In the above equation, $\mathbb{B}_{M11}$ is an $(M+1)\times(k+1)$ matrix as

$$\begin{bmatrix} 1 & 1 & 1 & 1 & \cdots & 1 \\ a_{k+1} & a_k & a_{k-1} & a_{k-2} & \cdots & a_1 \\ a_{k+2} & a_{k+1} & a_k & a_{k-1} & \cdots & a_2 \\ a_{k+3} & a_{k+2} & a_{k+1} & a_k & \cdots & a_3 \\ \vdots & \vdots & \vdots & \vdots & \ddots & \vdots \\ a_{2k} & a_{2k-1} & a_{2k-2} & a_{2k-3} & \cdots & a_k \\ a_{2k+1} & a_{2k} & a_{2k-1} & a_{2k-2} & \cdots & a_{k+1} \\ \vdots & \vdots & \vdots & \vdots & \ddots & \vdots \\ a_M & a_{M-1} & a_{M-2} & a_{M-3} & \cdots & a_{M-k} \\ a_{M+1} & a_M & a_{M-1} & a_{M-2} & \cdots & a_{M-k+1} \\ a_{M+2} & a_{M+1} & a_M & a_{M-1} & \cdots & a_{M-k+2} \\ \vdots & \vdots & \vdots & \vdots & \ddots & \vdots \\ a_{M+k-1} & a_{M+k-2} & a_{M+k-3} & a_{M+k-4} & \cdots & a_{M-1} \\ a_{M+k} & a_{M+k-1} & a_{M+k-2} & a_{M+k-3} & \cdots & a_M \end{bmatrix}$$

and $\mathbb{B}_{M12}$ is an $(M+1)\times(M-k)$ matrix as

$$\begin{bmatrix} 1 & 1 & 1 & 1 & 1 & \cdots & 1 & 1 \\ a_0 & & & & & & & \\ a_1 & a_0 & & & & & & \\ a_2 & a_1 & a_0 & & & & & \\ \ddots & \ddots & \ddots & & & & & \\ a_{k-1} & \cdots & a_2 & a_1 & a_0 & & & \\ a_k & a_{k-1} & \cdots & a_2 & a_1 & a_0 & & \\ & & & & \ddots & \ddots & \ddots & \\ a_{M-k-1} & a_{M-k-2} & \cdots & & a_3 & a_2 & a_1 & a_0 \\ a_{M-k} & a_{M-k-1} & \cdots & & & a_3 & a_2 & a_1 \\ a_{M-k+1} & a_{M-k} & \cdots & & & & a_3 & a_2 \\ & & & & \ddots & & & \ddots \\ a_{M-2} & a_{M-3} & \cdots & & a_{k+2} & a_{k+1} & a_k & a_{k-1} \\ a_{M-1} & a_{M-2} & \cdots & & a_{k+3} & a_{k+2} & a_{k+1} & a_k \end{bmatrix}$$

Equations (14) and (16) lead to

$$\vec{P}_M = \big(\mathbb{B}_{M1} - \mathbb{B}_{M2}\big)^{-1}\vec{b}_M \tag{19}$$

from which we obtain the state probabilities.

3. Statistics of the EIFA scheme

With the state probabilities in hands, the expected number of short frames in the data buffer at the STA can be approximated by

$$\bar{N} = \sum_{j=0}^{M} j P_j \tag{20}$$

with precision of ε.

The buffer overflow probability of the EIFA scheme is

$$\hat{p} = \sum_{j=B+1}^{M} P_j \tag{21}$$

where B is the buffer size measured in short frames.

4. Throughput

Now, we begin to measure the throughput in the EIFA scheme. Let L be the size of a frame (in bits).

In the case when there are n short frames in the data buffer at the STA, which happens with probability of P_n, we represent these frames by $\xi_1, \xi_2, \ldots, \xi_n$.

It holds that

$$n = m\,k + r \tag{22}$$

where m is a non-negative integer and r is such an integer that $0 \le r < k$.

We divide the above n frames into $m+1$ groups as $\{\xi_1, \xi_2, \ldots, \xi_k\}$, $\{\xi_{k+1}, \xi_{k+2}, \ldots, \xi_{2k}\}$, $\{\xi_{2k+1}, \xi_{2k+2}, \ldots, \xi_{3k}\}, \ldots, \{\xi_{(m-1)k+1}, \xi_{(m-1)k+2}, \ldots, \xi_{mk}\}$, and $\{\xi_{mk+1}, \xi_{mk+2}, \ldots, \xi_{n-1}, \xi_n\}$.

The last group is with r frames, but each of the other groups contains k frames. Thus, each group can be aggregated and transmitted in a single aggregation period. Hence, in the case when $r \neq 0$, i.e., integer n is not dividable by integer k, these n frames, which carry nL bits, cause the STA to totally consume $m+1$ aggregation periods and spend duration of $(m+1)T$ in data delivery. Additionally, in the case when $r=0$, it consumes m aggregation periods.

In summary, the STA expends $\lceil \frac{n}{k} \rceil T$ aggregation periods in delivering the n frames, where $\lceil \cdot \rceil$ is the ceil function. As a result, $nL/\left(\lceil \frac{n}{k} \rceil T\right)$ bits are delivered per unit of time.

Therefore, the expected throughput can be approximated with precision of ε by

$$\theta(k,T) = \sum_{n=1}^{M} P_n \frac{nL}{\lceil \frac{n}{k} \rceil T} = \frac{L}{T} \sum_{n=1}^{M} n P_n \frac{1}{\lceil \frac{n}{k} \rceil} \tag{23}$$

In the sequel, we refer to $\theta(k,T)$ as the approximated throughput.

5. Packet delay

Next, we study frame delay in the EIFA scheme. Delay of a frame is defined as the time interval from the instant when it arrives at the data buffer at the STA to the instant when it has been aggregated and transmitted. A frame may arrive at the buffer at any time in an aggregation period. Hence, the interval from the arrival time to the end of the aggregation period with duration of T takes a random value in $[0,T]$. We approximate it with the average of $T/2$. Thus, in the case when the frame arrives at the buffer having n buffered frames, its delay can be expressed by $\frac{T}{2} + \lceil \frac{n+1}{k} \rceil T$, where the second item stands for the time spent by the STA on aggregating and transmitting the previous n frames in the buffer, together with the newly arrived frame. Hence, the expected delay of the frame is approximated with precision of ε by

$$\tau(k,T) = T \sum_{n=0}^{M} P_n \left(\frac{1}{2} + \lceil \frac{n+1}{k} \rceil \right) \tag{24}$$

IV. Optimization Problem

To help our EIFA achieve the maximum throughput, we formulate the optimization problem in (25a) that maximizes the approximated throughput under the constraint on the approximated frame delay.

$$\max \theta(k,T) \quad \text{w.r.t.} \;\; k,T \tag{25a}$$

$$\text{s.t.} \;\; H + \frac{kL}{r} < T < \frac{k}{\lambda}, \tag{25b}$$

$$\tau(k,T) < d, \tag{25c}$$

$$k \in \{2,3,\dots,64\} \tag{25d}$$

Here, H stands for the sum of the time expended in contending for the channel, the preamble, headers of the physical layer and the MAC layer, and the frame check sequence (FCS), together with the time for receiving the ACK frame; r is the data rate applied by the STA in delivering the aggregated frame, i.e., a long frame consisting of up to k short frames.

In the above optimization problem, the constraint (25b) combines (1) with the equation $H + kL/r < T$, required for a long frame to be transmitted in one aggregation period. In constraint (25c), d is a preset constant as the upper bound of frame delay. And the constraint (25d) reflects how many short frames can be aggregated to generate a long frame, which is regulated in IEEE 802.11ax standard [7].

Next, we consider solving the optimization problem.

Let σ be a unit of time, say a millisecond (ms). Then, let

$$t_1 = \left\lceil \frac{1}{\sigma} \left(H + \frac{kL}{r} \right) \right\rceil \tag{26}$$

and

$$t_2 = \left\lfloor \frac{k}{\lambda \sigma} \right\rfloor \tag{27}$$

Here, t_1 and t_2 take the multiples of the time unit σ, and act as the lower bound and the upper bound for the variable T in Constraint (25b).

Then, the optimization problem is transformed into the following one with the variables k and T being positive integers.

$$\max \theta(k,T) \quad \text{w.r.t.} \;\; k,T \tag{28a}$$

$$\text{s.t.} \;\; k \in \{2,3,\dots,64\}, \tag{28b}$$

$$T \in \mathbb{T} = \{t_1, t_1+1, t_1+2, \dots, t_2\}, \tag{28c}$$

$$\tau(k,T) < d \tag{28d}$$

In the case when there are a few elements in the set $\mathbb{T}$ in (28c), the optimization problem (28a) can be solved by the exhaustive search. Otherwise, we can apply genetic algorithm that consists of selection, crossover, mutation operations [43], which is omitted due to space limitation.

V. Performance Evaluation

In this section, we evaluate performance of the proposed EIFA via simulation that mimics the OFDMA with UORA. The parameters applied in the simulation are shown in Table 1, where T_{tr} is the duration of a trigger frame, T_{SIFS} stands for short inter-frame space (SIFS), T_{pre} is the duration of preamble in the physical layer, T_{PHYhdr} is the duration of header of the physical layer, and T_{BA} represents the duration of block ACK. In the simulation, we mimic the duration of 10^7 short frame arriving to a STA.

Table 1. Parameters and values

Parameter	Value
r	200 Mbps
L	1500 Bytes
T_{tr}	100 µs
T_{SIFS}	16 µs
T_{pre}	36 µs
T_{PHYhdr}	40 µs
T_{BA}	40 µs
ε	0.01

The proposed EIFA is compared with the frame aggregation schemes “Maxk”, “Mink”, and “Randk”, where “Maxk” and “Mink” always let the STA choose the maximum NoS, i.e., 64, and the minimum NoS, i.e., 2, respectively, and “Randk” lets the STA randomly picks an NoS in the set $\{2,3,4,\dots,64\}$. Moreover, we also compare the EIFA with the two-level frame aggregation scheme, simply referred to as “Twolevel” scheme, presented in [34], which maximizes throughput. We set the bit error rate (BER) to 0 in the Twolevel scheme due to no BER considered in the EIFA. It should be pointed out that the Twolevel scheme assumes saturated traffic [34], which may not hold in practice.

Setting delay bound $d=0.01,\ 0.02,\ 0.03$ (s) and short frame arrival rate $\lambda=1000,3000,5000,7000,9000$ (in packets per second), we obtain the results shown in Figs.4, 5 and 6, where the Twolevel scheme does not consider delay bound d, i.e., every packet contributes to the throughput in the Twolevel scheme regardless of whether its delay is greater than d or not. Hence, the throughput surely takes a lower value if delay bound d is applied. This is because the packets with the delay longer than d are discarded.

It can be observed from Figs.4(a), 5(a) and 6(a) that EIFA outperforms the other schemes in throughput, which realizes the goal of the optimization problem in (25a). From these figures, we have the observation that the throughput in the Twolevel scheme improves when λ grows. In other words, heavier traffic brings in a higher throughput in the Twolevel scheme, which agrees with the saturated traffic assumption in the Twolevel.

Figs.4(b), 5(b), and 6(b) reflect the fact that the EIFA increases throughput at cost of packet delay. That is, the EIFA can tune the pair of parameters k and T such that throughput is improved while the preset delay bound is satisfied. It can be clearly seen from these figures that, for a given λ, the Twolevel scheme

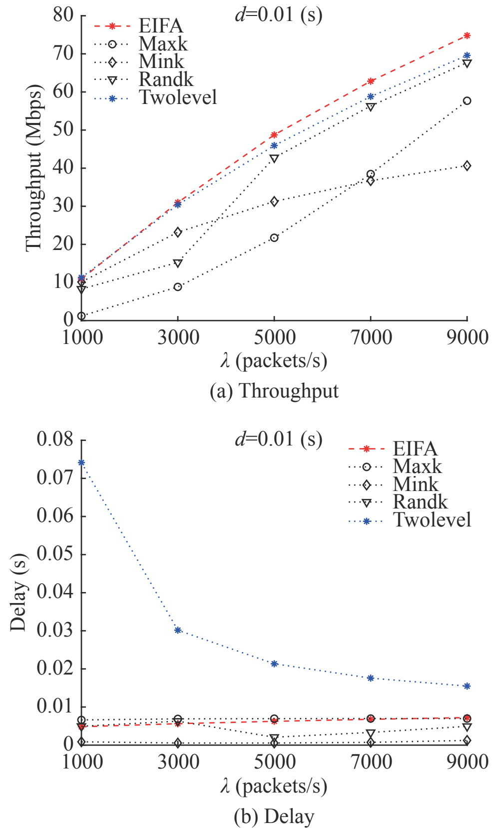

Fig. 4. Impact of packet arrival rate on throughput and delay ($d=0.01$ (s)).

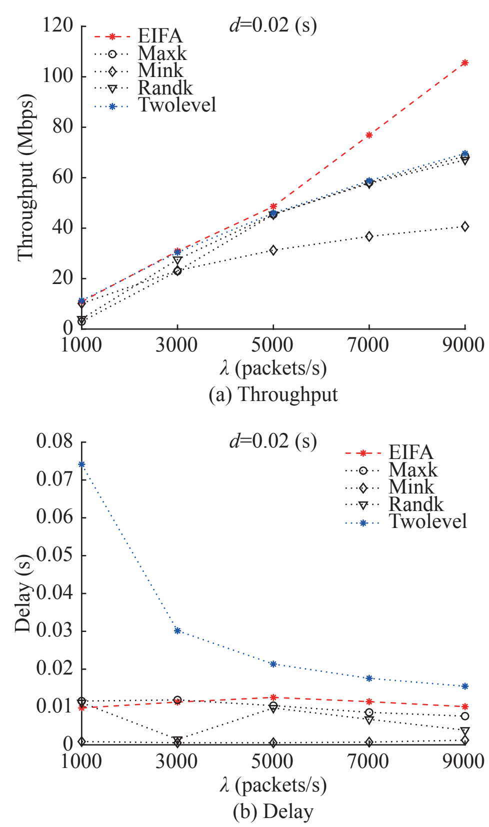

Fig. 5. Impact of packet arrival rate on throughput and delay ($d=0.02$ (s)).

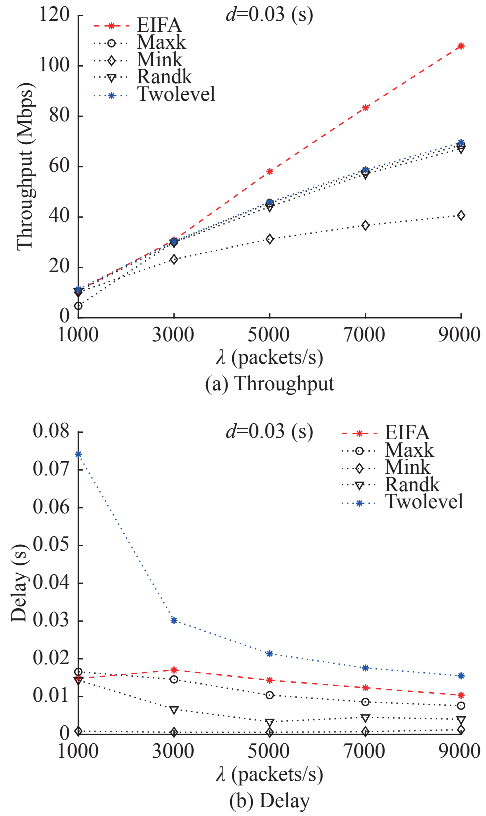

Fig. 6. Impact of packet arrival rate on throughput and delay ($d = 0.03$ (s)).

has delay larger than the other schemes, even larger than delay bound d in some cases. Therefore, the throughput in the Twolevel scheme will be much lower than the EIFA when delay bound d is applied in the Twolevel.

Impact of delay bound d on throughput in the EIFA is shown in Fig.7, from which we observe that, for a given λ, relaxing delay bound helps in improving throughput in the EIFA scheme. This agrees with our intuition that a higher delay bound enables the STA to have a longer waiting time for more short frames to come and thus more subframes can be aggregated into a longer frame, which increases efficiency of channel usage and improves throughput.

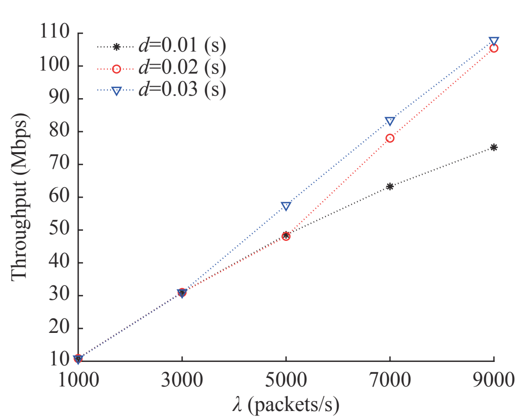

Fig. 7. Throughput vs. delay upper bound.

In summary, the proposed EIFA can improve throughput.

VI. Conclusions

Frame aggregation can improve throughput in the WLANs based on the family of IEEE 802.11 standard. The proposed EIFA scheme takes the new feature, i.e., the OFDMA mechanism, of the newest IEEE 802.11ax standard and enables the STAs in the 802.11ax WLANs to set the optimal NoS and waiting time in frame aggregation, which improves throughput. In this paper, we develop a novel Markov chain to model the one-level frame aggregation. In the future, we will investigate the Markov model for the two-level frame aggregation.

References

[1] IEEE Std 802.11-1997:1997, Information Technology-Telecommunications and Information Exchange Between Systems-Local and Metropolitan Area Networks-Specific Requirements Part 11: Wireless LAN Medium Access Control (MAC) and Physical Layer (PHY) Specifications, doi: 10.1109/IEEESTD.1997.85951.

[2] IEEE Std 802.15.4-2006:2006, IEEE Standard for Information Technology-Local and Metropolitan Area Networks-Specific Requirements-Part 15.4: Wireless Medium Access Control (MAC) and Physical Layer (PHY) Specifications for Low Rate Wireless Personal Area Networks (WPANs), doi: 10.1109/IEEESTD.2006.232110.

[3] S. Tozlu, M. Senel, W. Mao, *et al.*, "Wi-Fi enabled sensors for internet of things: A practical approach," *IEEE Communications Magazine*, vol.50, no.6, pp.134–143, 2012.

[4] Q. Q. Yang, G. Y. Zhou, W. H. Qin, *et al.*, "Air-kare: A Wi-Fi based, multi-sensor, real-time indoor air quality monitor," in *Proceedings of 2015 IEEE International Wireless Symposium (IWS 2015)*, Shenzhen, China, pp.1–4, 2015.

[5] R. R. Rajanna, S. Natarajan, and P. R. Vittal, "An IoT Wi-Fi connected sensor for real time heart rate variability monitoring," in *Proceedings of the 3rd International Conference on Circuits, Control, Communication and Computing (I4C)*, Bangalore, India, pp.1–4, 2018.

[6] M. Sivachitra, J. J. D. Kumar, R. Gokul, *et al.*, "Wi-Fi controlled multi-sensor robotic car," in *Proceedings of the 2nd International Conference on Artificial Intelligence and Smart Energy (ICAIS)*, Coimbatore, India, pp.1541–1546, 2022.

[7] IEEE Std 802.11ax-2021:2021, IEEE Standard for Information Technology-telecommunications and Information Exchange Between Systems Local and Metropolitan Area Networks-specific Requirements Part 11: Wireless LAN Medium Access Control (MAC) and Physical Layer (PHY) Specifications Amendment 1: Enhancements for high-efficiency WLAN, doi: 10.1109/IEEESTD.2021.9442429.

[8] D. J. Deng, Y. P. Lin, X. Yang, *et al.*, "IEEE 802.11ax: Highly efficient WLANs for intelligent information infrastructure," *IEEE Communications Magazine*, vol.55, no.12,

pp.52–59, 2017.

[9] IEEE, IEEE Std 802.11n^{TM} 2009:2009, IEEE Standard for Information Technology-Telecommunications and Information Exchange Between Systems-Local and Metropolitan Area Networks-Specific Requirements-Part 11: Wireless LAN Medium Access Control (MAC) and Physical Layer (PHY) Specifications, Amendment 5: Enhancements for Higher Throughput, New York, NY, USA: IEEE.

[10] D. Kotagiri, K. Nihei, and T. S. Li, "Distributed convolutional deep reinforcement learning based OFDMA MAC for 802.11ax," in *Proceedings of ICC 2021-IEEE International Conference on Communications*, Montreal, QC, Canada, pp.1–6, 2021.

[11] D. H. Xie, J. W. Zhang, A. M. Tang, *et al.*, "Multi-dimensional busy-tone arbitration for OFDMA random access in IEEE 802.11ax," *IEEE Transactions on Wireless Communications*, vol.19, no.6, pp.4080–4094, 2020.

[12] Y. Zheng, J. B. Wang, Q. H. Chen, *et al.*, "Retransmission number aware channel access scheme for IEEE 802.11ax based WLAN," *Chinese Journal of Electronics*, vol.29, no.2, pp.351–360, 2020.

[13] W. J. Lee, W. Shin, J. A. Ruiz-de-Azua, *et al.*, "NOMA-based uplink OFDMA collision reduction in 802.11ax networks," in *Proceedings of 2021 International Conference on Information and Communication Technology Convergence (ICTC)*, Jeju Island, Korea, Republic of, pp.212–214, 2021.

[14] L. Lanante, C. Ghosh, and S. Roy, "Hybrid OFDMA random access with resource unit sensing for next-gen 802.11ax WLANs," *IEEE Transactions on Mobile Computing*, vol.20, no.12, pp.3338–3350, 2021.

[15] R. G. Cheng, C. M. Yang, B. S. Firmansyah, *et al.*, "Uplink OFDMA-based random access mechanism with bursty arrivals for IEEE 802.11ax systems," *IEEE Networking Letters*, vol.4, no.1, pp.34–38, 2022.

[16] W. R. Ghanem, V. Jamali, Y. Sun, *et al.*, "Resource allocation for multi-user downlink MISO OFDMA-URLLC systems," *IEEE Transactions on Communications*, vol.68, no.11, pp.7184–7200, 2020.

[17] F. Khoramnejad, M. Rasti, H. Pedram, *et al.*, "Load management, power and admission control in downlink cellular OFDMA networks," *IEEE Transactions on Mobile Computing*, vol.20, no.4, pp.1477–1493, 2021.

[18] M. J. Xiao, L. S. Huang, K. Xing, *et al.*, "Opportunistic data aggregation in low-duty-cycle wireless sensor networks with unreliable links," *Chinese Journal of Electronics*, vol.22, no.3, pp.599–603, 2013.

[19] Y. X. Lin and V. W. S. Wong, "WSN01-1: Frame aggregation and optimal frame size adaptation for IEEE 802.11n WLANs," in *Proceedings of IEEE Globecom 2006*, San Francisco, CA, USA, pp.1–6, 2006.

[20] M. M. S. Kowsar and S. Biswas, "Performance improvement of IEEE 802.11n WLANs via frame aggregation in NS-3," in *Proceedings of 2017 International Conference on Electrical, Computer and Communication Engineering (ECCE)*, Cox's Bazar, Bangladesh, pp.1–6, 2017.

[21] S. Abdallah and S. D. Blostein, "Joint rate adaptation, frame aggregation and MIMO mode selection for IEEE 802.11ac," in *Proceedings of 2016 IEEE Wireless Communications and Networking Conference*, Doha, Qatar, pp.1–6, 2016.

[22] H. Assasa, A. Loch, and J. Widmer, "Packet mass transit: Improving frame aggregation in 60 GHz networks," in *Proceedings of the IEEE 17th International Symposium on A World of Wireless, Mobile and Multimedia Networks (WoWMoM)*, Coimbra, Portugal, pp.1–7, 2016.

[23] Y. Nomura, K. Mori, and H. Kobayashi, "Efficient frame aggregation with frame size adaptation for next generation MU-MIMO WLANs," in *Proceedings of the 9th International Conference on Next Generation Mobile Applications, Services and Technologies*, Cambridge, UK, pp.288–293, 2015.

[24] E. Charfi, L. Chaari, and L. Kamoun, "Joint urgency delay scheduler and adaptive aggregation technique in IEEE 802.11n networks," in *Proceedings of the 5th International Conference on Communications and Networking (COMNET)*, Tunis, Tunisia, pp.1–6, 2015.

[25] X. L. Zhou and A. Boukerche, "AFLAS: An adaptive frame length aggregation scheme for vehicular networks," *IEEE Transactions on Vehicular Technology*, vol.66, no.1, pp.855–867, 2017.

[26] M. Yazid and A. Ksentini, "Modeling and performance analysis of the main MAC and PHY features of the 802.11ac standard: A-MPDU aggregation vs spatial multiplexing," *IEEE Transactions on Vehicular Technology*, vol.67, no.11, pp.10243–10257, 2018.

[27] J. Saldana, J. Ruiz-Mas, and J. Almodóvar, "Frame aggregation in central controlled 802.11 WLANs: The latency versus throughput tradeoff," *IEEE Communications Letters*, vol.21, no.11, pp.2500–2503, 2017.

[28] J. Saldana, O. Topal, J. Ruiz-Mas, *et al.*, "Finding the sweet spot for frame aggregation in 802.11 WLANs," *IEEE Communications Letters*, vol.25, no.4, pp.1368–1372, 2021.

[29] A. Abedi, T. Brecht, and O. Abari, "Demystifying frame aggregation in 802.11 networks: Understanding and approximating optimality," *Computer Communications*, vol.180, pp.259–270, 2021.

[30] M. Morimoto, K. Sanada, H. Hatano, *et al.*, "Throughput and delay analysis for full-duplex WLANs with frame aggregation under non-saturated condition," in *Proceedings of the 22nd International Symposium on Wireless Personal Multimedia Communications (WPMC)*, Lisbon, Portugal, pp.1–5, 2019.

[31] K. Liu and C. L. Li, "An efficient adaptive frame aggregation scheme in vehicular Ad Hoc networks," in *Proceedings of the 9th International Conference on Wireless Communications and Signal Processing (WCSP)*, Nanjing, China, pp.1–6, 2017.

[32] S. Kim and J. H. Yun, "Efficient frame construction for multi-user transmission in IEEE 802.11 WLANs," *IEEE Transactions on Vehicular Technology*, vol.68, no.6, pp.5859–5870, 2019.

[33] J. L. Liu, M. W. Yao, and Z. L. Qiu, "Enhanced two-level frame aggregation with optimized aggregation level for IEEE 802.11n WLANs," *IEEE Communications Letters*, vol.19, no.12, pp.2254–2257, 2015.

[34] K. Suzuki and S. Yamazaki, "Throughput maximization based on optimized frame-aggregation levels for IEEE 802.11 WLANs," *IEEE Communications Letters*, vol.25,

no.5, pp.1725–1728, 2021.

[35] B. S. Kim, H. Y. Hwang, and D. K. Sung, "Effect of frame aggregation on the throughput performance of IEEE 802.11n," in *Proceedings of 2008 IEEE Wireless Communications and Networking Conference*, Las Vegas, NV, USA, pp.1740–1744, 2008.

[36] S. Seytnazarov, J. G. Choi, and Y. T. Kim, "Enhanced mathematical modeling of aggregation-enabled WLANs with compressed BlockACK," *IEEE Transactions on Mobile Computing*, vol.18, no.6, pp.1260–1273, 2019.

[37] I. Jabri, K. Mansour, I. Al-Oqily, *et al.*, "Enhanced characterization and modeling of A-MPDU aggregation for IEEE 802.11n WLANs," *Transactions on Emerging Telecommunications Technologies*, vol.33, no.1, article no.e4384, 2022.

[38] W. W. Lu, S. L. Gong, and Y. H. Zhu, "Timely data delivery for energy-harvesting IoT devices," *Chinese Journal of Electronics*, vol.31, no.2, pp.322–336, 2022.

[39] D. Skordoulis, Q. Ni, H. H. Chen, *et al.*, "IEEE 802.11n MAC frame aggregation mechanisms for next-generation high-throughput WLANs," *IEEE Wireless Communications*, vol.15, no.1, pp.40–47, 2008.

[40] Y. H. Zhu and V. C. M. Leung, "Efficient power management for infrastructure IEEE 802.11 WLANs," *IEEE Transactions on Wireless Communications*, vol.9, no.7, pp.2196–2205, 2010.

[41] Q. H. Chen and Y. H. Zhu, "Scheduling channel access based on target wake time mechanism in 802.11ax WLANs," *IEEE Transactions on Wireless Communications*, vol.20, no.3, pp.1529–1543, 2021.

[42] S. M. Ross, *Introduction to Probability Models*, 11th ed., Academic Press, New York, NY, USA, doi: 10.1016/C2012-0-03564-8, 2014.

[43] J. H. Holland, *Adaptation in Natural and Artificial Systems*, The MIT Press, Cambridge, MA, USA, 1992.

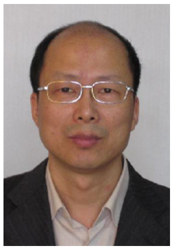

ZHU Yihua received the B.S. degree in mathematics from Zhejiang Normal University, Zhejiang, China, in July 1982; the M.S. degree in operation research and cybernetics from Shanghai University, Shanghai, China, in April 1993; and the Ph.D. degree in computer science and technology from Zhejiang University, Zhejiang, China, in March 2003. Dr. Zhu is a Professor at Zhejiang University of Technology, Hangzhou, Zhejiang, China. He is a Member of China Computer Federation Technical Committee on Internet of Things (IoT). His current research interests include IoT, WLANs, WSNs, RFID systems. He has served as Technical Program Committee Members or Co-chairs in the international conferences IEEE ICC, WCNC, GlobeCom, DCOSS, etc. (Email: yhzhu@zjut.edu.cn)

XU Mengying received the B.S. degree from Zhejiang A & F University, Zhejiang, China, in 2020. She is currently a candidate student for the M.S. degree in Zhejiang University of Technology. Her current research interests include channel access in the IEEE 802.11ax WLAN.